FULL PAPER

Synergetic Targeted Delivery of Sleeping-Beauty Transposon System to Mesenchymal Stem Cells Using LPD Nanoparticles Modified with a Phage-Displayed Targeting Peptide

*Kun Ma, Dong-Dong Wang, Yiyang Lin, Jianglin Wang, Valery Petrenko, and Chuanbin Mao**

An important criterion for effective gene therapy is sufficient chromosomal integration activity. The Sleeping Beauty (SB) transposon system is a plasmid system allowing efficient insertion of transgenes into the host genome. However, such efficient insertion occurs only after the system is delivered to nuclei. Since transposons do not have the transducing abilities of viral vectors, efficient delivery of this system first into cells and then into cell nuclei is still a challenge. Here, a phage display technique using a major coat displayed phage library is employed to identify a peptide (VTAMEPGQ) that can home to rat mesenchymal stem cells (rMSCs). A nanoparticle, called liposome protamine/DNA lipoplex (LPD), is electrostatically assembled from cationic liposomes and an anionic complex of protamine, DNA and targeting peptides. Various peptides are enveloped inside the LPD to improve its targeting capability for rMSCs and nuclei. The rMSC-targeting peptide and nuclear localization signal (NLS) peptide can execute the synergetic effect to promote transfection action of LPD. The homing peptide directs the LPD to target the MSCs, whereas the NLS peptide directs transposon to accumulate into nuclei once LPD is internalized inside the cells, leading to increased gene expression. This suggests that rMSC-targeting peptide and NLS peptide within LPD can target to rMSCs and then guide transposon into nuclei. After entering the nuclei, SB transposon increase the insertion rates into cellular chromosomes. The targeting LPD does not show obvious cell toxicity and influence on the differentiation potential of rMSCs. Therefore, the integration of SB transposon and LPD system is a promising nonviral gene delivery vector in stem cell therapy.

1. Introduction

The development of an ideal gene delivery system has been the goal of gene therapists for many years. Transgenic DNA must penetrate three biological barriers, namely, the cellular membrane, the nuclear membrane, and chromosomal integrity, for successful gene therapy. Gene delivery to mammalian chromosomes has been achieved using two broad classes of vectors, viral and nonviral.[1] Viruses efficiently deliver genes to target cells for expression as a part of their natural activity.[2] However, clinical outcomes in several gene therapy trials have served to highlight key problems of carcinomatous mutation in their therapeutic applications.[3,4,5] Nonviral vectors, as alternatives to viruses, are often less effective because the integration of single genes into chromosomes requires efficiently penetrating the above three barriers.[6,7]

Transposable elements can be considered as natural, nonviral gene delivery vehicles capable of efficient genomic insertion. The plasmid-based transposon system of Sleeping Beauty (SB) combines the advantages of viruses and naked DNA molecules.[8,9] The pDNA used in this work is a SB transposon system made of a SB transposase and a transposon that can insert a specific fragment of DNA into genomes of cells in a cut-and-paste fashion. Therefore, in contrast to conventional plasmid vectors, the transposon can be integrated into chromosomes through a precise, recombinase-mediated mechanism, providing long-term expression of the gene of interest in cells.[10] The advantages of transposons in comparison to viral systems include their simplicity and improved safety/toxicity profiles.[9] However, transposons play a role in promoting gene expression only after they can be delivered first across cell membrane and then into cell nuclei. In this work, we will integrate two peptides, a peptide that can target cell surface and another one that can target cell nuclei, into liposome-transposon complex for efficiently delivering transposon to cell nuclei for enhanced gene expression. The

K. Ma, D.-D. Wang, Y. Lin, J. Wang, Prof. C. B. Mao
Department of Chemistry and Biochemistry
University of Oklahoma
Stephenson Life Sciences Research Center
101 Stephenson Parkway, Norman, OK 73019, USA
E-mail: cbmao@ou.edu
Dr. V. Petrenko
Department of Pathobiology
Auburn University
Auburn, AL 36849, USA

DOI: 10.1002/adfm.201102963

© 2013 WILEY-VCH Verlag GmbH & Co. KGaA, Weinheim

liposome-transposon complex, termed liposome protamine/DNA lipoplex (LPD), is a nanoparticle made by mixing a cationic liposome and an overall anionic preformed complex of anionic DNA, cationic protamine, anionic cell-surface targeting peptides (identified by phage display) and cationic nuclear localization signal (NLS) peptide. Such LPD system can allow the transgenic DNA to penetrate the aforementioned three biological barriers for successful gene delivery.

Phage display technique is a promising method for identifying interacting peptide ligands to certain targets without knowledge about their molecular properties.[11] In vitro and in vivo phage display applications have been successfully conducted to identify homing peptide ligands targeting various cells or tissues.[12,13] In this work, a peptide was screened by a phage display to increase the targeted delivery of transposon to rat mesenchymal stem cells (rMSCs). During the screening process, a phage library, made of millions of phage clones (input) with each clone displaying a unique peptide on the major coat, was allowed to interact with rMSCs. The phage clones that do not bind to the cell surfaces are washed away by using a washing buffer. Then, an elution buffer was used to remove the phage clones bound to the cell surface. The eluted phage clones (output) are amplified by infecting bacterial cells and used as a new input to interact with rMSCs again. This screening process where the output is used as a new input was repeated for a few rounds. The phage DNA can be sequenced to determine the foreign peptides displayed on the phage clones that bind to cell surface and survive the screening process.

Mesenchymal stem cells (MSCs) have the capacity to differentiate into cells of mesodermal lineages, including osteogenic, chondrogenic, myogenic and adipogenic lineages. This differentiation capacity makes the use of MSCs an attractive treatment for tissue regeneration and engineering. Furthermore, they are relatively easy to isolate, manipulate and culture, and, at least in vitro, show significant expansion capability.[14,15] These characteristics make them very interesting candidates for the delivery of exogenous genes. We expected that the identification of a novel rMSC-homing peptide by phage display screening would enable novel design and preparation of efficient gene carriers, which could deliver the transposon into rMSCs specifically. In order to overcome the nuclear membrane, we also used an NLS peptide to enhance nuclear translocation of gene materials. The basic NLS peptide is derived from the simian virus 40 large tumor antigen (DKKKRKV), which mediates binding of the karyophilic protein to importin α. The NLS peptide was found to be vital in achieving the high levels of gene expression.[16] In the present study, we used phage display technique to identify an rMSC-homing peptide ligand and then integrated both the identified homing peptide and the reported NLS peptide into a peptide-combined liposome-based carrier for the development of an effective SB transposon gene delivery system.

Table 1. Peptide sequences displayed by selected rMSC-binding phage clones and their occurrence frequencies.

Motif Sequence	Frequency
VTAMEPGQ	28
AFNPEPGQ	11
VTALEPGQ	7
DTPPGWDQ	5

2. Results

2.1. Identification of rMSC-Homing Phage Clones

rMSC-homing phage clones were isolated from a major coat displayed phage library after three rounds of panning. The major coat displayed phage library, also termed landscape phage library, is made of billions of fd-tet phage clones with each phage clone fully displaying a unique foreign peptide on the major coat. Namely, for each phage clone, the foreign peptide is fused to each of the ≈3900 copies of major coat protein of fd-tet phage. Phages that were bound to rMSCs in the initial selection procedure were amplified separately by infecting bacteria and used as an input for the next round of affinity selection. After the three rounds of affinity selection, clones were randomly picked and sequenced. The cell-binding peptides and their frequencies are shown in **Table 1**. No cell internalized phages were detected after cell lysate amplification and phage titering. The cell-binding phage clones with a sequence of VTAMEPGQ demonstrated the highest affinity to rMSCs. Phage capture ELISA also indicated that the selected cell-binding phage with sequence VTAMEPGQ has high affinity against rMSCs (**Figure. 1**).

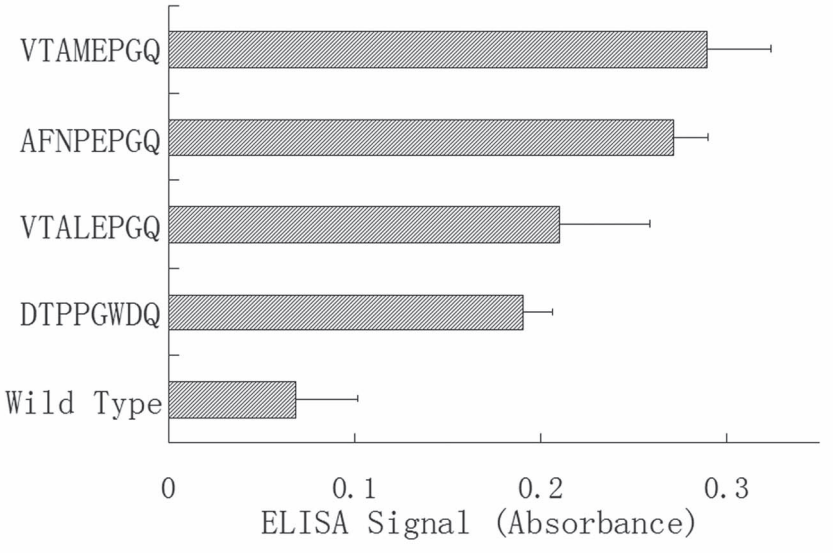

Figure 1. Binding of control wild type phage and affinity selected phages to rMSCs evaluated by ELISA. The *x* axis indicates the absorbance of ELISA signal and the *y* axis shows the affinity selected peptide sequences displayed on the major coat of phage.

© 2013 WILEY-VCH Verlag GmbH & Co. KGaA, Weinheim

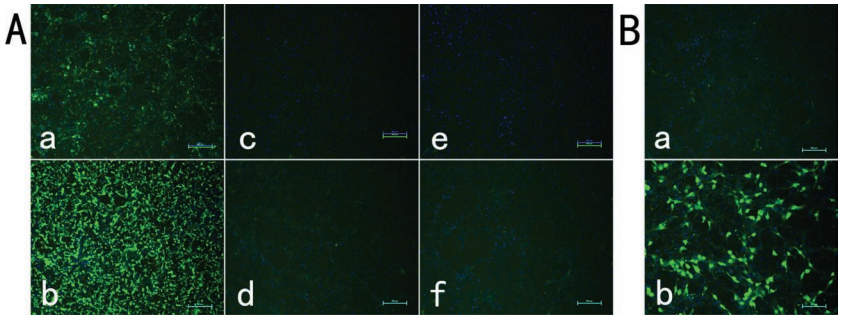

Figure 2. Affinity and specificity of peptide 1 with rMSCs. A) Testing the interaction of dye-labled peptide 1 or 4 with rMSCs and control cells: strong fluorescence signals were visualized, indicating that a large amount of 10 μM FITC-labeled peptide 1 was located in rMSCs (b). Weak fluorescence was detected from 1 μM FITC-labeled peptide 1 in rMSCs (a). No specific fluorescence signal was observed from either 1 and 10 μM FITC-labeled control peptide 4 (c, d). No specific fluorescence signal was observed on rat fibroblastic cells (e) or rat smooth muscle cells (f) after incubated with 10 μM FITC-peptide 1, suggesting FITC-labeled peptide was not associated with the cells. B) Testing the blocking of binding to rMSCs in the presence of peptide 1 or 4. rMSCs were preincubated with 10 μM peptide 1 (a) or 4 (b) without FITC followed by incubation with 10 μM FITC-labeled peptide 1. Fluorescence microscopy confirmed that rMSCs preincubated with peptide 4 displayed much stronger fluorescence signals (b) than those preincubated with peptide 1 (a). The nuclei were stained with DAPI. Scale bar: 100 μm.

2.2. rMSC-affinity and Specificity of the Identified Peptide

The identified peptide (VTAMEPGQ) was designated as peptide 1 (Table 1). A random peptide (GCVKYMVM, peptide 4) was used as a negative control. The rMSCs were incubated with FITC labeled peptide 1 or 4, and observed under a fluorescence microscope. When incubated with 10 μM FITC-peptide 1, strong fluorescent signals were observed in rMSCs (**Figure 2**A(b)), whereas a weak FITC signal was detected from the cells when incubated with 1 μM FITC-peptide 1 (Figure 2A(a)). When incubated with 1 and 10 μM FITC-labeled control peptide 4, no specific fluorescence signal was observed from rMSCs at both concentrations (Figure 2A(c,d)). This result suggests that peptide 1 can bind with rMSCs in a concentration dependent way. However, the random peptide 4 cannot bind to rMSCs specifically. To further investigate the affinity of peptide 1 to other cell types, rat fibroblastic cells and rat smooth muscle cells were used as control cells and incubated with 10 μM FITC-peptide 1. The result showed that peptide 1 bound to neither rat fibroblastic cells (Figure 2A(e)) nor rat smooth muscle cells (Figure 2A(f)), which indicated its specificity against rMSCs.

2.3. Competitive Binding Using Synthetic Peptide

In order to verify whether internalization of peptide 1 takes place through a VTAMEPGQ recognition motif, competitive assay was performed by prebinding of peptide 1 or 4 without FITC to rMSCs. Peptide 1 or 4 was incubated with the cells prior to the incubation of FITC-labeled peptide 1. Figure 2C shows that preincubation with unlabeled peptide 1 reduced the binding of FITC-labeled peptide 1 to the rMSCs, but the preincubation with peptide 4 did not affect the binding of FITC-labeled peptide 1 with rMSCs. This fact confirms that FITC-labeled peptide 1 is competitively inhibited in the presence of peptide 1, but not of peptide 4.

2.4. Preparation and Physico-Chemical Properties of Liposome Protamine/DNA Lipoplexes (LPD)

To construct the LPD, we used a two-step packaging technology employing a multilayering method.[17,18] First, the DNA was packaged into a condensed core via electrostatic interactions with protamine. The targeting peptide with slightly positive potential was also added and interacted with the plasmid to form a negatively charged particle. Second, positively charged DOTAP/DOPE/Chol liposome was added to form a complex with negative protamine/DNA particle, leading to the formation of LPD (**Figure 3**).

The formation of LPD was verified via gel electrophoresis and zeta potential measurement. According to the results of gel electrophoresis, DNA migration started to be retarded when the weight ratio of protamine to pDNA reached 1.5:1 for the protamine to condense the DNA (Figure S1, Supporting Information). Thus, the protamine/pDNA particle was prepared at a weight ratio of 1:1 to ensure that its zeta potential was negative to favor its integration with the DOTAP/DOPE liposome.

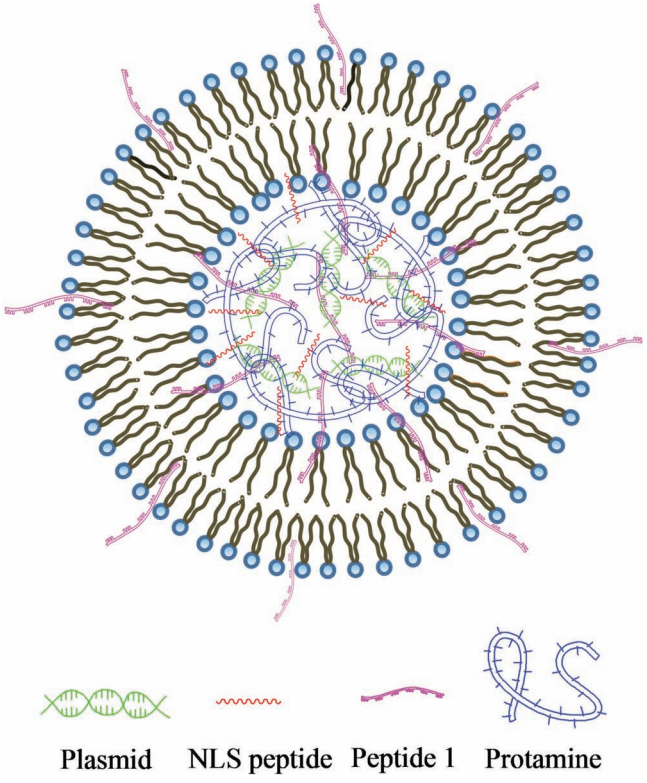

Figure 3. Schematic illustration of targeting LPD modified with rMSC-homing peptide (peptide 1) and NLS peptide.

© 2013 WILEY-VCH Verlag GmbH & Co. KGaA, Weinheim

Table 2. Particle size and zeta potential of protamine/pDNA particles and LPD. The pDNA concentration was 20 μg/mL. The concentration of liposome is denoted by the concentration of DOTAP in LPD.

	Size [nm]	Zeta-potential [mV]
Protamine:pDNA = 1:1	245.7 ± 6.47	–27.55 ± 3.33
Protamine:pDNA = 1.5:1	118.5 ± 4.99	26.25 ± 2.99
LPD (10 mM liposome)	245.1 ± 5.65	20.74 ± 1.89

The results of dynamic light scattering (DLS) showed that the zeta potential of the protamine/pDNA complex was negative and 245.7 nm in size at the weight ratio of 1:1 (**Table 2**), which was consistent with the result of gel electrophoresis. At a weight ratio of 1.5:1, the particle of protamine/pDNA became positive in potential and 118.5 nm in size, which indicates that pDNA was condensed by protamine to form a more compact particle.

The LPD was then prepared with various concentrations of liposome. The gel electrophoresis and DLS were both performed to verify the formation of the LPD. With the increasing concentration of liposome, DNA migration was retarded gradually (Figure S2, Supporting Information). The protamine/pDNA particles could be complexed completely with DOTAP/DOPE liposome at a concentration of 10 mM DOTAP. The results of DLS were consistent with those of the gel electrophoresis. After being incorporated with the DOTAP/DOPE liposome, LPD had a zeta potential of positive 20.74 mV, and was 245.1 nm in size (Table 2). The size of the LPD was confirmed by TEM (**Figure 4**).

2.5. Transfection Efficiency

To investigate the peptide-enabled targeted delivery efficiency, we performed the transfection efficiency study using LPD with the synthetic targeting peptide 1. Lipofectamine 2000 served as a control (**Figure 5**A). The result showed that the transfection efficiency of LPD with peptide 1 was 3.24- and 1.41-fold higher than Lipofectamine2000 and LPD without peptide, respectively, showing enhanced targeted gene delivery to rMSCs. This indicates that peptide 1 enhanced transgenic expression by means of targeting to rMSCs. This demonstrated the great potential of peptide 1 as a ligand in rMSCs targeting.

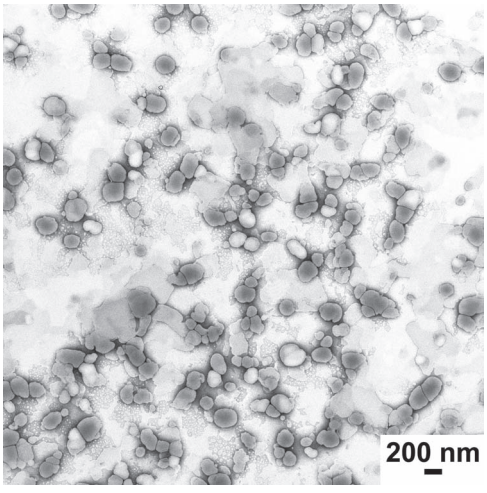

Figure 4. Morphology of LPD observed by transmission electron microscope. The particles were negatively stained by 2% uranyl acetate for 3 min.

To further enhance the nuclear translocation efficiency of SB transposon system, three-fold reiterated NLS motif (DPKKKRKVDPKKKRKVDPKKKRKV, peptide 2) of SV40 T large antigen was employed to promote the gene expression of LPD.[19] To investigate the effect of fused peptide, an LPD with a fusion peptide (DPKKKRKVDPKKKRKVDPKKKRKV-VTAMEPGQ, peptide 3) from peptides 1 and 2 was compared to the LPD containing unfused peptides 1 and 2. The results showed that LPD with fusion peptide 3 did not demonstrate a better gene expression than sole peptide 1 or 2. This means that after fusion, peptides 1 and 2 did not produce an improved effect. However, LPD with both unfused peptides 1 and 2 integrated could obtain the highest gene expression among all the peptides combinations. This indicates that a synergetic effect could be realized by encapsulating both peptides 1 and 2 in LPD. The fluorescence microscopy results also confirmed this synergetic effect (Figure 5B).

The LPD with various combinations among the peptides 1, 2, and 3 was then investigated for a higher transgenic efficiency (**Figure 6**A). The result showed that the combination of peptides 1 and 2 was still better than the other two combinations. The effects of varying peptide/plasmid weight ratio on transfection efficiencies into rMSCs were determined to ascertain an optimal dosage. Using a 3:1 peptide to plasmid ratio resulted in the best gene expression among all examined peptide/plasmid ratios (Figure 6B). A decreased transfection efficiency of LPD was observed at ratios higher or lower than the 3:1 of peptide/plasmid ratio. It was therefore concluded that using a 3:1 peptide/plasmid ratio was optimal for further use.

To verify the effect of peptides 1 and 2, the random peptide (GCVKYMVM, peptide 4) was utilized as a substitution and combined with either peptide 1 or 2 in LPD for gene transfection. The results showed that compared to peptides 1 and 2, the random peptide did not increase any transfection efficiency of LPD in rMSCs (Figure 6C). After being combined with peptide 1 or 2, peptide 4 still did not result in an improved transfection efficiency. It further confirmed that there was a synergetic effect between peptides 1 and 2, i.e., between rMSC-homing and NLS peptide. These two peptides should be co-existing (but without forming fusion peptide) to maximize the transfection efficiency of LPD.

A time course of gene expression was then performed for SB transposon system (made of pT2/EGFP and pSB11 at a mass ratio of 2:1) and pEGFP-N1 genes with expression levels measured up to 168 h (Figure 6D). After 96 h, the transgenic expression level of SB transposon system in rMSCs reached its maximum, which was referred to as 100%. After 24 h, relatively low SB transposon system and pEGFP-N1 transfection rates of only about 50% of maximum of transposon transfection were observed. Transfection of pEGFP-N1 reached its maximum at 72 h, which was only about 70% of the transposon system's maximum, and with no further significant increase seen at 96 h. The transfection rates of pEGFP-N1 then decreased

© 2013 WILEY-VCH Verlag GmbH & Co. KGaA, Weinheim

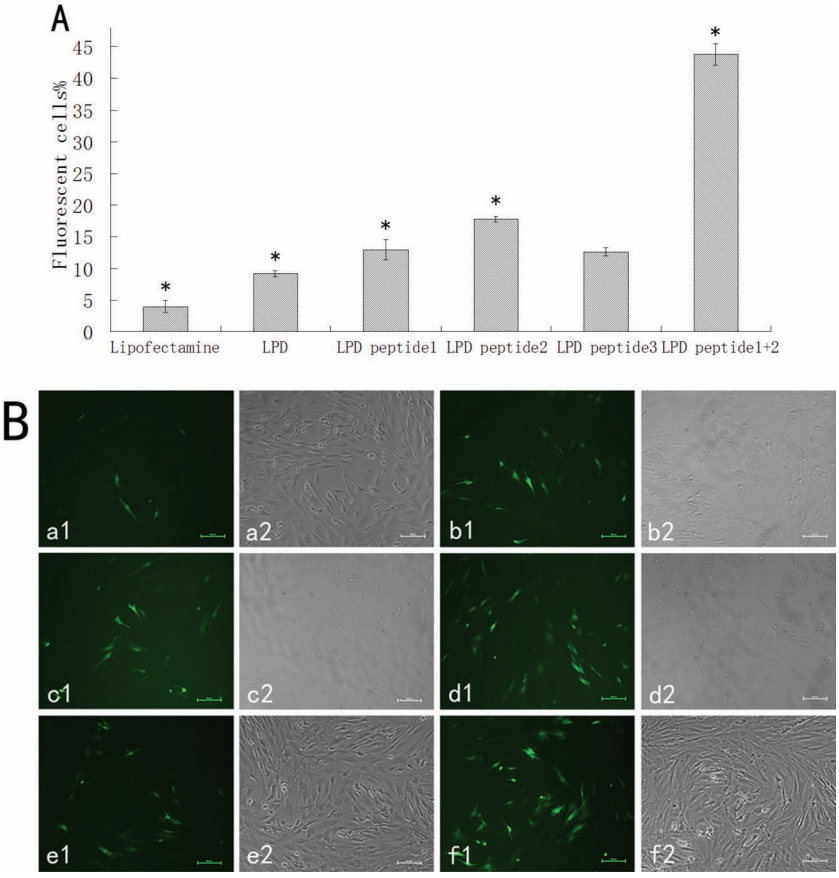

Figure 5. Transfection efficiency of LPD in rMSCs. Lipofectamine 2000 was used as the control. A) EGFP expression after transfection by LPD with various peptides was examined by flow cytometry. LPD with both unfused peptides 1 and 2 integrated could obtain the highest gene expression among all peptides tested. Fusion peptide 3 (fused from peptides 1 and 2) did not display a better gene expression. The percentage of EGFP positive cells is shown as the mean ± standard deviation of triplicate measurements. (*) indicates a statistically significant difference ($p < 0.05$). B) Comparison of transfection expression of EGFP mediated by Lipofectamine2000 (a), LPD (b), and LPD with peptide 1 (c), peptide 2 (d), peptide 3 (e), peptide 1 + 2 (f) in rMSCs using the transposon containing EGFP reporter gene. Image 1 in (a–f) shows GFP expression and image 2 is the corresponding bright-field light image. Scale bar: 100 μm.

significantly to approximately 50% after 144 and 168 h. The transposon system did not show obvious decreases in transfection levels at 120, 144, and 168 h, which are all maintained at about 90% of the maximum.

2.6. Confocal Microscopy

For investigating the intracellular localization of LPD with or without NLS peptide, carboxyfluorescein labeled DOPE was used to prepare liposome. The pDNA was labeled with rhodamine. The cells were scanned with a confocal fluorescence microscope. It was revealed that after the cells were transfected with LPD containing the NLS peptide, rhodamine-labeled pDNA colocalized with the nuclei as indicated by white arrows in **Figure 7**A(d). However, LPD without the NLS peptide rarely translocated pDNA into the nuclei (Figure 7B). This result indicates that the NLS peptide guides the nuclear translocation of pDNA efficiently. This efficient translocation into the nucleus may be responsible for the high transfection efficiency of LPD.

2.7. Cytotoxicity

In vitro cytotoxicity of various concentrations of LPD and Lipofectamine 2000 was investigated with rMSCs after 12 h incubation at 37 °C by MTT assay (**Figure 8**). At Lipofectamine 2000 concentrations over 40 mM, cell viability was lower than 80%, indicating that it has obvious toxicity at these higher concentrations. Cell viability was slightly reduced at higher concentrations of LPD, but still higher than 80%. This fact demonstrates that LPDs with peptides show low cytotoxicity with good biocompatibility. Furthermore, there was no significant difference in the toxicity of different formulation at all given concentrations ($p < 0.05$).

2.8. Cell Differentiation

Osteogenesis of rMSCs after transfected by LPD was determined by the production of LPD after 14 days in an osteogenic medium. Osteopontin is a bone marker protein and its expression by osteoblasts differentiated from rMSCs was used as a marker to verify the osteoblastic differentiation of rMSCs. Similar to untransfected rMSC (**Figure 9**B) but unlike the undifferentiated control (Figure 9C), LPD-transfected rMSCs (Figure 9A) retained the ability of rMSCs to differentiate along the osteogenic lineage.

3. Discussion

MSCs are multipotent cells, which hold a tremendous promise for the construction and regeneration of tissues. However, MSCs by themselves have exhibited limited efficacy in terms of tissue regeneration and differentiation to the desired cell types. Therefore, genetic engineering has been proposed as a method to enhance the efficacy of MSC-based therapies. Genetic modification of stem cells by transposons to obtain sustained gene expression may further enhance their therapeutic efficacy.

Sleeping Beauty (SB) is a Tc1/mariner-like transposon system, artificially reconstructed by site-directed mutagenesis from an inactive salmonid transposable element.[20] After expression in a cell, SB transposases bind to the SB inverted/direct repeat elements (IRs/DRs) in a substrate-specific manner and induce transposition by a "cut-and-paste" mechanism, inserting a transposon into a new genomic location containing TA dinucleotides.[20,21] Transposon integration occurs with little

© 2013 WILEY-VCH Verlag GmbH & Co. KGaA, Weinheim

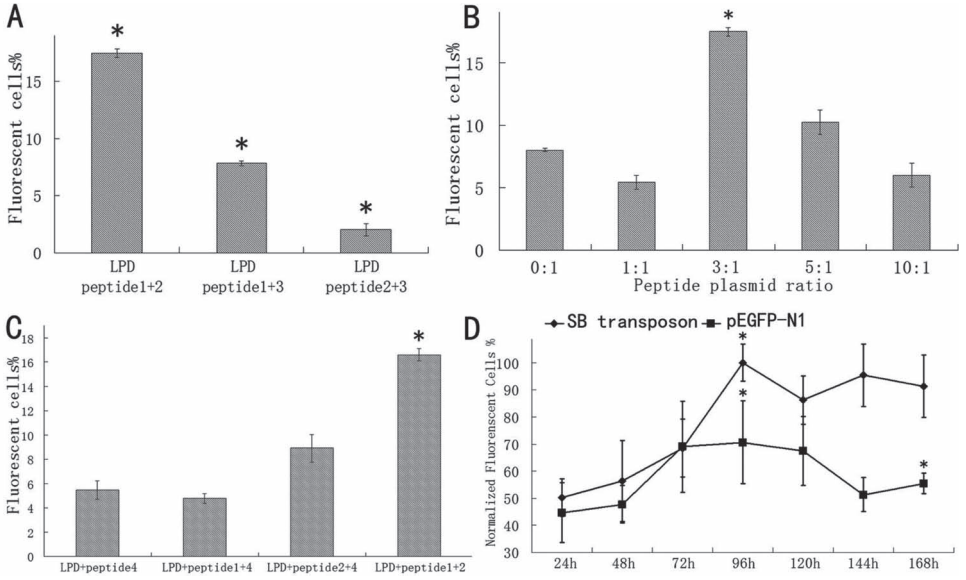

Figure 6. A) The EGFP expression level of LPD with different combinations of the peptides 1, 2, and 3. The combination of peptides 1 and 2 was superior to the other two combinations. B) The transfection efficiency of LPD with the various peptide/plasmid weight ratios. LPD with peptide/plasmid ratio of 3:1 was optimal for gene expression. C) A control peptide (peptide 4) was utilized to verify the synergetic effect between peptides 1 and 2. Peptide 4 did not promote transfection of LPD neither solely nor combining with peptide 1 or 2. D) Percentage of EGFP positive cells in rMSCs after varying the duration of transgene expression. The highest transfection levels were observed at 96 h with the SB transposon system gene, which was set as 100%. SB transposon system maintained about 90% of its maximum after 168 h. However, pEGFP-N1 showed obvious decreases in transfection levels at that time. Each assay was shown as means ± standard deviation (n = 3). (*) Indicates a statistically significant difference ($p < 0.05$).

preference for the transcriptional status or genetic identity of the sequence into which the SB transposon integrates.[21–24] Since its introduction, the SB transposon system has been tested in numerous model organisms to correct several genetic deficiencies.[25]

Although proof-of-principle studies using nonviral gene delivery have established the potential of SB-mediated insertion into the host genome for long-term gene correction,[26] the delivery is nonselective. Thus, an efficient cell type-specific targeting system is desirable to fully investigate the potential of SB and other vertebrate transposon vector systems for gene therapy.

We constructed LPD for a targeted transposon delivery. This structure is advantageous in terms of integrating various functional devices for controlling intracellular trafficking into one nanoparticle. The LPD was a nanoparticle formed solely by charge-charge interactions, specifically, between preformed cationic liposomes, and an anionic complex of protamine, targeting peptides and anionic nucleic acids. First, the plasmid was condensed by protamine into a negatively charged compact core. The complex should only contain the required amount of protamine that can provide sufficient concentration but keep the complex negatively charged. Then, the complex interacted with the cationic liposome to form the LPD. Again, the LPD should only contain a slight excess of lipids that allow full coating of the complex with the cationic lipids. (Figure 3)

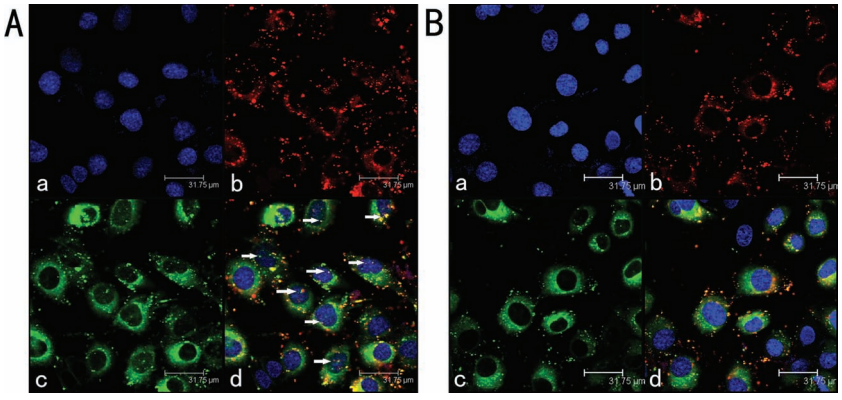

Figure 7. Subcellular distribution of LPD with and without NLS peptide 2 (A and B, respectively) was visualized by confocal microscopy in rMSCs. a: DAPI labeled nuclei (blue); b: rhodamine labeled pDNA (red); c: carboxyfluorescein labeled liposome (green); d: merged images of a, b, and c. Guided with NLS peptide, LPD and rhodamine-labeled pDNA could colocalize in the nuclei. However, without NLS peptide, LPD and pDNA rarely appeared into the nuclei. Scale bar: 31.75 µm. White arrows in A(d) are used to indicate that rhodamine-labeled pDNA colocalized with the nuclei.

According to the result of zeta-potential measurement, protamine/pDNA particle at a 1:1 weight ratio had a negative potential. After being incorporated with DOTAP/DOPE/Chol liposome, the zeta potential of particles was shifted to positive, which confirmed the formation of LPD (Table 2). The gel electrophoresis, which was consistent

© 2013 WILEY-VCH Verlag GmbH & Co. KGaA, Weinheim

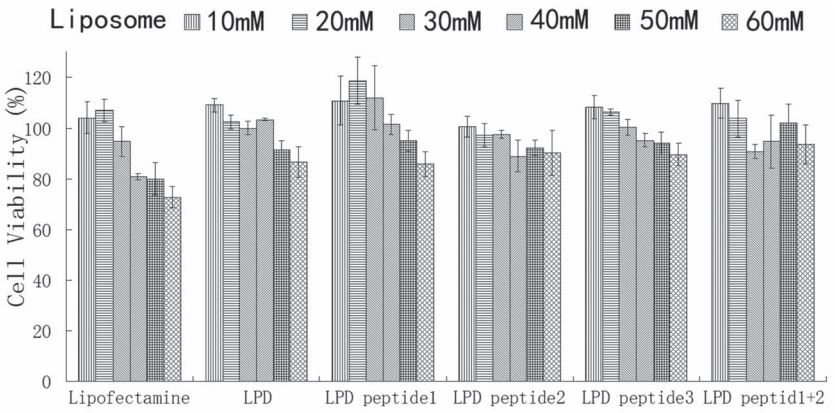

Figure 8. MTT assay for evaluating cytotoxicity of LPD with various peptides at different liposome concentrations. Lipofectamine 2000 was used as a control. The cell viability of samples with LPD with peptides at all liposome concentrations was higher than 80%. Lipofectamine 2000 had obvious toxicity at concentrations over 40 mM. The concentration of liposome is denoted by the concentration of DOTAP in LPD. The data points represent the mean ± standard deviation of three experiments.

with zeta potential measurement, also demonstrated the shift of zeta-potential (Supporting Information, Figure S1 and Figure S2). The highly positively charged surface of LPD (zeta potential ≈20 mV) would favor the strong charge-charge interaction with the cells, which could increase the association with the cells during gene transfection. The diameter of LPD was approximately 200 nm, which would facilitate its endocytosis by cells (Figure 4).[27]

Three rounds of consecutive phage display panning were conducted to select peptide ligands which can target rMSCs specifically. After panning, four peptide sequences were identified from randomly selected individual recombinant phages (Table 1). Based on the recovery efficiency and phage capture ELISA results (Figure 1), we categorized the peptide VTAMEPGQ as the best binder to rMSCs under stringent conditions. rMSCs-affinity assay showed that as the concentration of peptide increases, more FITC-labeled peptide 1 was located in rMSCs, but neither high nor low concentrations of control peptide 4 induced localization into rMSCs (Figure 2A). Furthermore, the affinity between dye-labeled peptide 1 and rMSCs was competitively inhibited in the presence of peptide 1. However, the affinity of dye-labeled peptide 1 for rMSCs was not affected by control peptide 4 (Figure 2B). After the FITC-labeled peptide 1 was interacted with two different control cells (rat fibroblastic cells and rat smooth muscle cells) separately, we found that peptide 1 did not bind any of the two control cells (Figure 2A(e,f)). These facts confirm that peptide 1 has high targeting specificity and affinity against rMSCs. Thus, we selected peptide 1 as rMSCs-homing peptide candidate for the rest of our study.

The transfection experiment showed that transgenic activity of LPD could be promoted by either peptide 1 or 2. This indicates that peptide 1 could target to rMSCs and enhance the endocytosis of LPD mediated by receptor. The peptide 2 could direct plasmid into the nuclei to improve the interaction between the exogenous gene and the host genome. Peptide 3 is fused from peptides 1 and 2 and did not display better

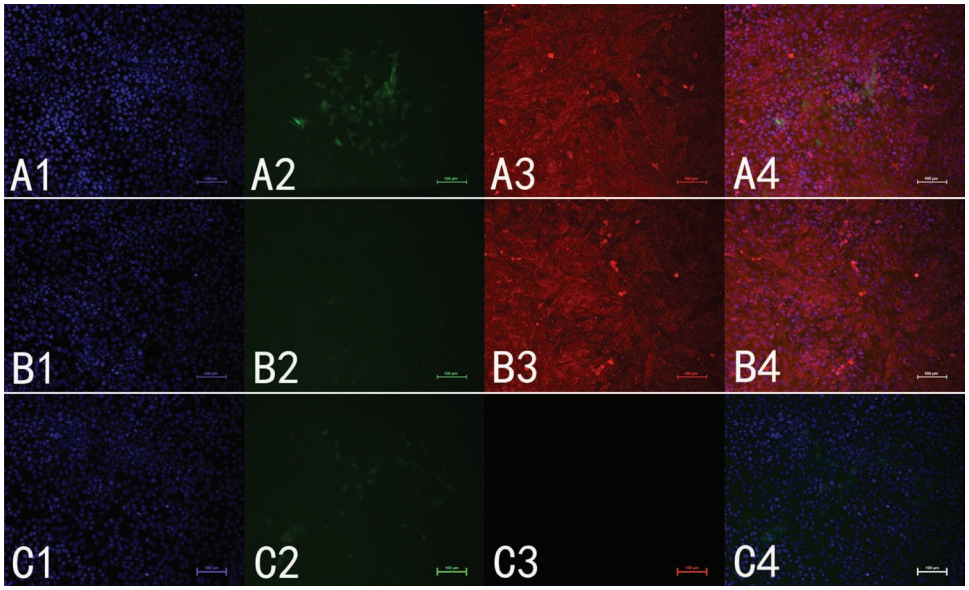

Figure 9. Osteogenic differentiation assays of rMSCs. A) Differentiation of LPD-transfected rMSCs in an osteogenic medium. B) Differentiation of untransfected rMSCs in an osteogenic medium. C) The undifferentiated rMSC was tested as a control. Image 1 in (A–C) shows cell nuclei using DAPI stain (blue); image 2 is GFP expression (green); image 3 shows immunofluorescence staining of osteopontin-positive cells (red); image 4 is merged from images 1, 2, and 3. No differences in osteogenic differentiation were observed between transfected and untransfected rMSCs, but the differentiation of both transfected and untransfected rMSCs was different from the undifferentiated control. Scale bar: 100 µm.

© 2013 WILEY-VCH Verlag GmbH & Co. KGaA, Weinheim

action than the original sequences (Figure 5). It is assumed that the function of the two peptides might be degraded by steric hindrances after being fused together, thus resulting in their inactivity.

After being combined with both unfused peptides 1 and 2, LPD mediated a higher gene expression. It was suggested that LPD could firstly home to and enter the rMSCs by means of peptide 1, and then, be guided by peptide 2 to translocate into the nuclei and achieve efficient gene delivery. The two peptides executed their actions at the right space and time, resulting in a synergetic effect. Other combinations of the three peptides did not show the optimal transfection action as shown by peptides 1 and 2 (Figure 6A).

To verify the synergetic effect of peptides 1 and 2, one of them was replaced with the control peptide 4 for the combination. The control peptide 4 did not possess any function to improve transfection. Moreover, the peptide 4 also could not execute a synergetic effect with either peptide 1 or 2 (Figure 6C). This demonstrates that peptides 1 and 2 could assist each other exclusively to achieve optimal transgenic action.

It was shown that the optimal transgenic action can be completed at a 3:1 peptide plasmid ratio (Figure 6B). This suggests that a lower quantity of peptide could not execute its function to target the cell and nucleus efficiently. Additionally, when the quantity of the peptide is too high, its receptor might be blocked, resulting in a depressed targeting transposition. This phenomenon is the so-called "excess inhibition" of receptors.

Confirmation of the delivery of transposon into the nuclei by LPD was supported by confocal microscopy. This result showed that LPD with peptides 1 and 2 can accumulate into nucleus efficiently (Figure 7) but when LPD was modified with only peptide 1, the plasmid failed to translocate into the nucleus. This fact suggests that the NLS peptide contributes to the efficient nuclear localization of the complexes. The nuclear localization is very important for transposon transfection. Since transposons do not have the transducing abilities of viral vectors, it is necessary to devise a method to deliver this plasmid-based system into cells efficiently. The transposition rate is critically dependent on the efficiency of uptake of the plasmids into the cell nuclei. After being guided into the nucleus by NLS, transposon had a high opportunity to integrate into host genome, causing a greatly increased transfection efficiency.

One of the major barriers of nonviral gene delivery is the transient nature of gene expression. Therefore, stable genomic integration is a particularly attractive feature to enable stable transduction of dividing target cells, especially for stem cells, and their differentiated progeny. We performed a time course of gene expression levels using transposon. The levels of gene expression were examined up to 168 h both from pEGFP-N1 and transposon in rMSCs. For the pEGFP-N1, a gradually reduced expression level was observed after 96 h. However, the transposon maintained 90% of its maximum transfection even after 168 h, which appeared to increase the duration of gene expression. The transgenic activity of transposon was also superior to the pEGFP-N1 as 1.43 times (Figure 6D). This suggested that the expression of the SB transposase gene on transposition rates will trigger the activity of SB transposon to increase insertion rates of transgenes into cellular chromosomes.[28] Thus, the transposon system could yield unprecedented stable and durative gene transfer efficiencies that compare favorably to the stable transduction efficiencies of integrating viral vectors.[29,30] This system is expected to facilitate widespread applications in functional genomics and gene therapy.

It was shown that LPD was relatively safer than Lipofectamine 2000. No notable toxicity was observed for LPD among any of the given concentrations. This might result from the biocompatibility of liposomes and peptides (Figure 8). LPD was found to have no negative effect on the differentiation potential of rMSCs. Cells transfected with the LPD were able to differentiate into the osteogenic lineage as were the untransfected cells (Figure 9). Thus, LPD with various peptides was regarded as a safe gene delivery system. Furthermore, it can be utilized over a larger range of dosages. Accordingly, LPD is a promising gene carrier without any significant adverse effects on the rMSCs.

4. Conclusions

We identified an rMSC-targeting peptide by phage display. A liposome protamine/DNA lipoplex (LPD) was constructed by combining the targeting peptide and a nuclear localization signal (NLS) peptide with a Sleeping Beauty transposon delivery system. Our results show that the selected peptide can improve the transfection efficiency due to its rMSC-targeting property. The rMSC transfections mediated by LPD with the targeting peptide and NLS peptide were much more efficient than those mediated by the randomly chosen control peptide. We also found that the targeting peptide and NLS peptide could have a synergetic effect to promote efficient and lasting transfection expression of transposon. Furthermore, LPD neither showed apparent cytotoxicity nor disturbed the osteogenic differentiation of rMSCs. Therefore, a liposome-based nanoparticle combined with NLS and rMSC-homing peptide was developed for targeted delivery of the transposon system to rMSCs, yielding stable and durative gene transfer efficiency, making it a promising gene carrier for future applications.

5. Experimental Section

Plasmid Development: The original SB transposon pT2/SVNeo and transposase pSB11 were a gift from Dr. Perry B. Hackett (University of Minnesota). The neomycin resistance gene in pT2/SVNeo was converted into the EGFP gene by restriction digestion with *Bcl* I and *BstB* I (New England Biolabs, Inc. MA, USA). The fragment excised by the two restriction enzymes from pT2/SVNeo plasmids was discarded and replaced by a PCR fragment of pEGFP-N1 with a similar restriction digestion. The sequence of primer 1 is GCGGTGATCATATGGTGAGCAAGGGC; the primer 2 is GCGGTTCGAACTTTACTTGTACAGCT. After the appropriate fragments were gel purified and recovered, the EGFP fragment was cloned by ligation into the pT2/SVNeo, giving rise to pT2/EGFP constructs. pT2/EGFP and pSB11 plasmid were purified using the EndoFree Plasmid Max Kit (Qiagen, CA, USA). Rhodamine-labeling for pDNA was performed using a ITTM-Rhodamine labeling kit (Mirus, Madison, WI, USA) according to the manufacturer's protocol.

Phage Display Panning: The phage display screening procedure followed the previous protocol with a slight modification.[31] We used a major coat displayed phage library, called landscape phage library, to conduct the biopanning. This library contains billions of fd-tet phage clones and in each phage clone the foreign peptide is displayed on the N-terminal end of each copy of major coat protein of fd-tet phage. Briefly,

© 2013 WILEY-VCH Verlag GmbH & Co. KGaA, Weinheim

the landscape phage library was first depleted with culture flask at 37 °C for 1 h to remove the phages that specifically bound to the culture flask. The depleted phage library was incubated with target rMSCs at room temperature for 1 h. The rMSCs were washed 10 times with bovine serum albumin (BSA)/Tween washing buffer to remove the unbound phages. The cell bound phages were eluted with low pH elution buffer (0.1N HCl, 1 mg/mL BSA and pH adjusted to 2.2 with glycine) for 10 min. The eluate was neutralized by 1 M Tris-HCl (pH = 9.1) immediately. The first-round eluate was concentrated by using a Centricon 100 kDa Ultrafilter (Amicon, USA). The concentrated eluate was transfected to the starved cells and incubated for 15 min at room temperature. The phage-infected cells were added to NZY medium with tetracycline (0.2 μg/mL) and incubated for 45 min at 37 °C with shaking. The tetracycline concentration was increased to 20 μg/mL, and the shaking of the flask was continued for 24 h at 37 °C. The rMSC-internalized phage clones were recovered using the cell lysis buffer (2% sodium deoxycholate, 10 mM Tris-HCl, 2 mM EDTA, pH 8.0). The cells were centrifuged at 130 g for 10 min. The supernatant was removed and the cell lysis buffer was added to the pellet. The phages were used for amplification and further selection as stated above. The purified phage after each round was used as an input library for the next round of selection, which proceeded similarly to the first round as described above. After the third round of the selection, the eluted phages were titrated and 40 random colonies were picked up for sequencing in order to determine the sequence of rMSC-binding peptides.

Binding Assessment by Phage Capture ELISA: The binding ability and specificity of the selected phages to rMSCs were measured by enzyme linked immunosorbent assay (ELISA). Confluent cells in 24-well plate (Corning Inc., MA, USA) were fixed by 4% paraformaldehyde (Sigma-Aldrich Co. LLC, USA) for 15 min, blocked with 0.1% BSA for 1 h at room temperature, and washed three times with PBS. Subsequently, 2×10^9 cfu purified phages in blocking buffer were added and incubated for 1 h at room temperature. The plate was subsequently washed three times with PBS containing 0.5% Tween 20, and washed another three times with PBS. This was followed by incubation with anti-fd bacteriophage IgG conjugated with alkaline phosphatase (Abcam, MA, USA) for 1 h at room temperature. After a final washing step, alkaline phosphatase substrate, p-nitrophenyl phosphate, was added to the wells and the absorbance was measured at 405 nm using a plate reader (Gen5, BioTek Instruments, Inc. USA).

Peptide-Affinity Assay: The peptide-affinity assay was performed according to the method mentioned previously with minor modifications.[32,33] The cells were cultured until 70–90% confluence, and then incubated with 1 and 10 μM FITC-labeled peptide 1 or 4 for 4 h at 37 °C to allow cell binding. The cells were fixed with 4% paraformaldehyde for 30 min at 4 °C. The rat fibroblastic cells and rat smooth muscle cells were used as control cells. They were incubated with 10 μM FITC-labeled peptide 1 for 4 h at 37 °C to investigate the specificity of peptide 1. The nuclei were then counterstained with DAPI. The cells were observed under a Nikon fluorescence microscope.

Competitive Binding Using Synthetic Peptide: For specific competitive blocking of peptide, rMSCs (Invitrogen, USA) were cultured with peptide 1 or control peptide 4 (GCVKYMVM) without FITC at a concentration of 10 μM for 2 h. After incubation, 10 μM of FITC-labeled peptide 1 was added and incubated for another 4 h. Then the cells were then examined by fluorescence microscopy.

The Preparation and Physico-Chemical Properties of Liposome Protamine/DNA Lipoplexes (LPD): LPD was prepared according to the method reported previously with some modifications.[17,18,34] First, the liposomes consisting of DOTAP, DOPE and cholesterol (1:1:1 molar ratio) (Avanti Polar Lipids, Inc. USA) were prepared by thin film hydration. Second, protamine (0.5 mg/mL) (Sigma-Aldrich Co. LLC, USA), various peptides (0.5 mg/mL), and the Sleeping Beauty system (pDNA, a mixture of transposon and transposase gene at a mass ratio of 2:1) were mixed at various weight ratios. The resultant protamine/pDNA complex was allowed to stand at room temperature for 20 min. The above liposome was then added into the protamine/pDNA complex followed by vortexing. The resultant mixture was kept at room temperature for another 20 min to form LPD.

Protamine/pDNA particles were prepared at different weight ratios, and LPD was prepared with various liposome and peptide concentrations. The samples were electrophoresed on a 0.8% (w/v) agarose gel in TAE buffer at 90 V for 40 min, and analyzed on a UV illuminator to show the location of the DNA.

The size and zeta-potential values of protamine/pDNA particles and LPD were determined by dynamic light scattering (DLS) (Zeta Potential Analyzer, Brook haven Instruments Corporation, Holtsville, NY). The final concentration of pDNA was 20 μg/mL in HEPES buffer for assay.

The morphology of LPD was observed using TEM (Carl Zeiss, Germany). One drop of LPD was placed on a copper grid and stained with 2% uranyl acetate for 3 min. The grid was allowed to dry further for 20 min and then examined with the electron microscope.

Transfection Efficiency: For the transfection experiments, rMSCs were seeded in the 24-well plate at a density of 1×10^5 cells/well and incubated overnight. The pDNA was made of a mixture of transposon pT2/EGFP and transposase pSB11 with a mass ratio of 2:1 as described in an earlier report.[35] The LPD with various peptides in low glucose DMEM was added, and Lipofectamine2000 (Invitrogen, USA) was used as a control. The cells were incubated for 4 h at 37 °C. The transfection medium was then replaced with a fresh culture medium and the cells were further incubated for up to 72 h. Inverted fluorescent microscopy was also used to observe the GFP expression. The transfected cells was digested by trypsin and fixed in a 4% paraformaldehyde for 30 min at 4 °C to prepare single-cell suspensions. The percentage of cells positive for GFP was determined by flow cytometry (Becton-Dickinson Biosciences, Franklin Lakes, NJ, USA) by setting a gate according to the control and 10 000 cells were evaluated in each experiment.

Confocal Microscopy: For confocal microscopy, LPD was prepared by carboxyfluorescein-labeled DOPE (Avanti Polar Lipids, Inc. USA), and the pDNA was labeled with rhodamine as mentioned above. The rMSCs were grown on glass cover slips in 12-well plates and incubated at 37 °C for a day. The cells were then transfected by labeled LPD and pDNA complexes. The cells were then incubated for 4 h at 37 °C. The transfection medium was then replaced with a fresh medium. After 5 h, the cells were fixed with 4% paraformaldehyde for 30 min. To stain the cell nuclei, the cells were incubated with DAPI for 30 min at 4 °C, and then the cover slips were mounted on glass slides. The fluorescence was examined with a confocal laser scanning microscope (Leica TCS NT, Germany).

Cytotoxicity Assay: Cytotoxicity of LPD was assayed using MTT reagent. Briefly, rMSCs were seeded at 10 000 cells per well in 96-well plates. One day later, the cells were transfected by LPD with various peptides at different liposome concentration. The Lipofectamine 2000 was used as the control. The cells were incubated for another 12 h at 37 °C. The medium was replaced with 80 μL of fresh medium without serum and 20 μL of MTT (5 mg/mL) (Sigma-Aldrich Co. LLC, USA) solution, and incubated for an additional 4 h. Subsequently, the medium was removed and 100 μL of dimethyl sulfoxide (DMSO) was added. The absorbance at 570 nm was measured by using a microplate reader.

Osteogenesis Assay: 1×10^5 transfected or untransfected MSCs/well were seeded in a 24-well plate in triplicate. After 24 h, medium was removed and 500 μL of HyClone osteogenic differentiation medium (Thermo Fisher Scientific Inc., USA) was added. Medium was changed every 3 days. Cultures were harvested at day 14. To analyze osteopontin expression, cells were fixed with 4% paraformaldehyde. Cells were saturated with 5% BSA for 30 min. 300 μL of anti-osteopontin antibody (ab 8448-200, Abcam, MA, USA), which was diluted 1:300 in phosphate buffered saline (PBS) containing 5% BSA, was added and incubated overnight at 4 °C. The cells were then washed with PBS/5% BSA and incubated with a secondary, tetramethylrhodamine goat anti-rabbit IgG (H+C) (Molecular probes, Invitrogen, USA) for 60 min at room temperature. The nuclei were stained by DAPI. The cells were observed with a fluorescence microscope.

Statistics Analysis: For statistical analysis, one-way analysis of variance (ANOVA) was carried out by SPSS 11 software, and a p values < 0.05 were considered statistically significant.

© 2013 WILEY-VCH Verlag GmbH & Co. KGaA, Weinheim

Supporting Information

Supporting Information is available from the Wiley Online Library or from the author.

Acknowledgements

K.M. and D.-D.W. contributed equally to this work. This work was in part supported by National Institutes of Health (R01HL092526-01A2, R03AR056848-01 and 1R21EB015190-01A1). We would like to thank the National Science Foundation (CBET-0854465, CBET-0854414, CBET-1229309, DMR-0847758), Oklahoma Center for Adult Stem Cell Research (434003), and Oklahoma Center for the Advancement of Science and Technology (HR11-006) for the financial support. We would also like to thank Dr. Antoni Tomsia at Lawrence Berkeley National Laboratory for help during experiments as well as his grant support from National Institutes of Health (5R01DE01563309). Finally, we thank Dr. Gopal Abbineni, Dr. Haibao Zhu, Dr. Jim C. Henthorn, and Dr. Kenneth J. Dormer for their kind help during the experiments.

Received: July 12, 2011
Revised: April 12, 2012
Published online: October 9, 2012

[1] W. F. Anderson, *Nature* **1998**, *392*, 25.
[2] R. O. Snyder, *J. Gene Med.* **1999**, *1*, 166.
[3] D. W. Pack, A. S. Hoffman, S. Pun, P. S. Stayton, *Nat. Rev. Drug Discovery* **2005**, *4*, 581.
[4] E. Marshall, *Science* **2002**, *298*, 34.
[5] S. E. Raper, N. Chirmule, F. S. Lee, N. A. Wivel, A. Bagg, G. P. Gao, J. M. Wilson, M. L. Batshaw, *Mol. Genet. Metab.* **2003**, *80*, 148.
[6] I. M. Verma, N. Somia, *Nature* **1997**, *389*, 239.
[7] M. Nishikawa, L. Huang, *Hum. Gene Ther.* **2001**, *12*, 861.
[8] P. B. Hackett, S. C. Ekker, D. A. Largaespada, R. S. McIvor, *Adv. Genet.* **2005**, *54*, 187.
[9] T. Sumiyoshi, N. G. Holt, R. P. Hollis, S. Ge, P. M. Cannon, G. M. Crooks, D. B. Kohn, *Hum. Gene Ther.* **2009**, *20*, 1607.
[10] X. Xue, X. Huang, S. E. Nodland, L. Mátés, L. Ma, Z. Izsvák, Z. Ivics, T. W. LeBien, R. S. McIvor, J. E. Wagner, X. Zhou, *Blood* **2009**, *114*, 1319.
[11] G. P. Smith, *Science* **1985**, *228*, 1315.
[12] M. A. Arap, *Genet. Mol. Biol.* **2005**, *28*, 1.
[13] M. K. Yoo, S. K. Kang, J. H. Choi, I. K. Park, H. S. Na, H. C. Lee, E. B. Kim, N. K. Lee, J. W. Nah, Y. J. Choi, C. S. Cho, *Biomaterials* **2010**, *31*, 7738.
[14] Y. Gafni, G. Turgeman, M. Liebergal, G. Pelled, Z. Gazit, D. Gazit, *Gene Ther.* **2004**, *11*, 417.
[15] H. K. Vaananen, *Ann. Med.* **2005**, *37*, 469.
[16] M. A. Zanta, P. Belguise-Valladier, J. P. Behr, *Proc. Natl. Acad. Sci. USA* **1999**, *96*, 91.
[17] S-D., Li, S. Chono, L. Huang, *J. Controlled Release* **2008**, *126*, 77.
[18] T. Masuda, H. Akita, K. Niikura, T. Nishio, M. Ukawa, K. Enoto, R. Danev, K. Nagayama, K. Ijiro, H. Harashima, *Biomaterials* **2009**, *30*, 4806.
[19] M. Hoare, U. Greiser, S. Schu, K. Mashayekhi, E. Aydogan, M. Murphy, F. Barry, T. Ritter, T. O'Brien, *J. Gene Med.* **2010**, *12*, 207.
[20] Z. Ivics, P. B. Hackett, R. H. Plasterk, Z. Izsvak, *Cell* **1997**, *91*, 501.
[21] Z. Izsvak, Z. Ivics, *Mol. Ther.* **2004**, *9*, 147.
[22] S. R. Yant, X. Wu, Y. Huang, B. Garrison, S. M. Burgess, M. A. Kay, *Mol. Cell Biol.* **2005**, *25*, 2085.
[23] A. M. Geurts, C. S. Hackett, J. B. Bell, T. L. Bergemann, L. S. Collier, C. M. Carlson, D. A. Largaespada, P. B. Hackett, *Nucleic Acids Res.* **2006**, *34*, 2803.
[24] C. Berry, S. Hannenhalli, J. Leipzig, F. D. Bushman, *PLoS Comput. Biol.* **2006**, *2*, e157.
[25] P. B. Hackett, D. A. Largaespada, L. J. Cooper, *Mol. Ther.* **2010**, *18*, 674.
[26] P. B. Hackett, *Mol. Ther.* **2007**, *15*, 10.
[27] E. Oh, J. B. Delehanty, K. E. Sapsford, K. Susumu, R. Goswami, J. B. Blanco-Canosa, P. E. Dawson, J. Granek, M. Shoff, Q. Zhang, P. L. Goering, A. Huston, I. L. Medintz, *ACS Nano* **2011**, *5*, 6434.
[28] L. R. Belur, J. L. Frandsen, A. J. Dupuy, D. H. Ingbar, D. A. Largaespada, P. B. Hackett, R. Scott McIvor, *Mol. Ther.* **2003**, *8*, 501.
[29] J. B. Bell, E. L. Aronovich, J. M. Schreifels, T. C. Beadnell, P. B. Hackett, *Mol. Ther.* **2010**, *18*, 1796.
[30] E. H. Lin, M. Keramidas, C. Rome, W. T. Chiu, C. W. Wu, J. L. Coll, W. P. Deng, *Biomaterials* **2011**, *32*, 1978.
[31] G. Abbineni, S. Modali, B. Safiejko-Mroczka, A. V. Petrenko, C. Mao, *Mol. Pharmaceutics* **2010**, *7*, 1629.
[32] Y. Pi, X. Zhang, J. Shi, J. Zhu, W. Chen, C. Zhang, W. Gao, C. Zhou, Y. Ao, *Biomaterials* **2011**, *32*, 6324.
[33] K. A. Kelly, N. Bardeesy, R. Anbazhagan, S. Gurumurthy, J. Berger, H. Alencar, R. A. Depinho, U. Mahmood, R. Weissleder, *PLoS Med.* **2008**, *5*, 657.
[34] S-D. Li, L. Huang, *Ann. N. Y. Acad. Sci.* **2006**, *1082*, 1.
[35] R. L. Belur, K. Podetz-Pedersen, J. Frandsen, R. S. McIvor, *Nat. Protoc.* **2007**, *2*, 3146.

© 2013 WILEY-VCH Verlag GmbH & Co. KGaA, Weinheim